Layered structure around an extended gliding discharge column in a methane-nitrogen mixture at high pressure

Kong, Chengdong; Gao, Jinlong; Li, Zhongshan; Aldén, Marcus; Ehn, Andreas

Published in:
Applied Physics Letters

DOI:
10.1063/1.5097908

2019

Document Version:
Publisher's PDF, also known as Version of record

Applied Physics Letters

Layered structure around an extended gliding discharge column in a methane-nitrogen mixture at high pressure

Cite as: Appl. Phys. Lett. **114**, 194102 (2019); https://doi.org/10.1063/1.5097908
Submitted: 29 March 2019 • Accepted: 29 April 2019 • Published Online: 15 May 2019

Chengdong Kong, Jinlong Gao, Zhongshan Li, et al.

Applied Physics Letters ARTICLE scitation.org/journal/apl

Layered structure around an extended gliding discharge column in a methane-nitrogen mixture at high pressure

Cite as: Appl. Phys. Lett. **114**, 194102 (2019); doi: 10.1063/1.5097908
Submitted: 29 March 2019 · Accepted: 29 April 2019 ·
Published Online: 15 May 2019

Chengdong Kong,[a] Jinlong Gao, Zhongshan Li, Marcus Aldén, and Andreas Ehn

AFFILIATIONS

Division of Combustion Physics, Lund University, P.O. Box 118, S-221 00 Lund, Sweden

[a]Author to whom correspondence should be addressed: kongcd1987@gmail.com

ABSTRACT

The current work aims at investigating the detailed spatial structure of the thin plasma column of a gliding arc (GA) discharge extended in N_2-CH_4 gas mixtures, using visualization techniques. The GA discharge was operated at up to 5 atm in a high-pressure vessel with extensive optical access. The results show that the emission intensity from the plasma column increased tenfold with the addition of 0.1% CH_4 in nitrogen, compared to that in pure N_2. Furthermore, an additional layer located around the GA discharge column is detected. Imaging through spectral filters and spectral analysis of the emitted signal indicate that the emissions of this outer layer are mostly from the CN A-X and CH A-X transitions. This outer layer can propagate and extinguish dynamically, similar to the flame front in combustion. Besides, the separation of this outer layer to the plasma core decreases with pressure. The layered structure and its dynamical behaviors can be explained by a plasma-sustained radical propagation mechanism. The high-power plasma column can produce a high-temperature zone with rich atomic species, surrounded by the relatively cold N_2-CH_4 mixture. At the mixing layer between the high-temperature zone and the N_2-CH_4 mixture, some highly exothermic reactions occur to produce excited CN and CH species, which emit their specific spectra. As the high-temperature zone expands with time, the outer layer propagates outward. However, with the propagation continuing, the radical species involved in the outer layer formation are rapidly consumed, and thus, this layer disappears when it propagates too far away from the plasma column.

Gliding arc (GA) discharge is an easy-handling and low-cost scheme to produce nonthermal high-power plasma in a large volume at high pressure ($\geq$1 atm),[1–3] and thus, it has numerous potential applications in combustion assistance,[4] surface treatment,[5] fuel reforming,[6] and chemical synthesis.[7] There have been plenty of reports on the physical and chemical characteristics of GA discharge.[8–11] However, for any specific application, the gas mixtures of the GA discharge can be unique and so are the discharge characteristics. GA discharges in air and argon have been extensively investigated by experiments[9,12–15] and modeling,[16–20] while GA discharge in the methane (CH_4)-nitrogen (N_2) mixture is rarely reported. There were some references about dielectric barrier discharge (DBD),[21] radio frequency,[22] low-pressure glow,[23] and microwave[24] discharges in N_2-CH_4 mixtures to study the chemical kinetics in the discharge and afterglow processes. As for the GA discharge, only one group used the rotating gliding arc plasma to activate methane for hydrogen production in a N_2-CH_4 mixture.[6,25] They presented much information about the emission spectra and the main produced species in the afterglow and also proposed detailed kinetic models. However, the spatially resolved morphologies of the GA discharge column were not demonstrated. Therefore, knowledge of the GA discharge plasma column in the N_2-CH_4 mixture is still missing.

In this investigation, we report a finding of a layered structure around the GA discharge column in well-controlled nitrogen-methane gas mixtures. The plasma column of GA discharge is anchored on electrodes, which are installed in a high-pressure chamber and visualized by spatiotemporally resolved techniques [including intensified charged-coupled device (ICCD) camera, imaging spectrometer, and high-speed camera]. By increasing the gas pressure up to 5 atm, the high-pressure GA discharge is achieved and the pressure effect on discharge characteristics is explored.

Figure 1 shows a schematic of the experimental apparatus used in this work. A pair of diverging electrodes to support the gliding arc discharge is installed on a Teflon plate inside a high-pressure chamber,

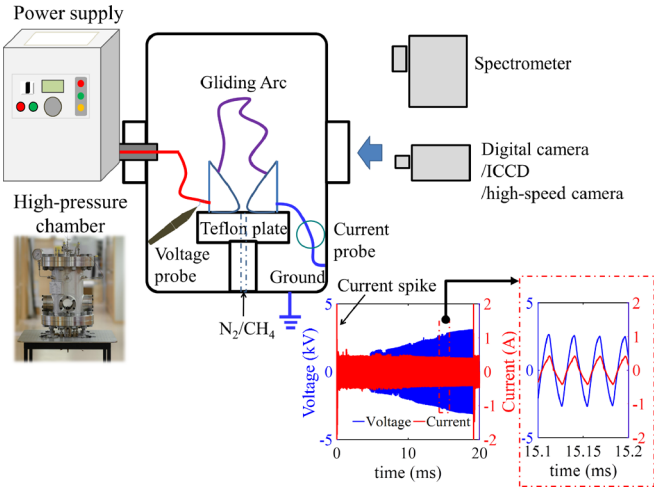

FIG. 1. Schematic of the experimental setup, together with a typical current-voltage waveform.

which was built to provide an elevated pressure environment from atmospheric pressure to 35 atm. The details about this high-pressure vessel can be found in Ref. 26. One of the electrodes is connected to an AC power supply (Generator 9030 E, SOFTAL Electronic GmbH) through an insulated connector on the wall of the chamber, whereas the other electrode is connected to the chamber wall, which is grounded. Three broadband antireflection coated sapphire windows provide optical access for the discharge inside the chamber. Various techniques including a digital camera (D7100, Nikon) equipped with a microNikon lens (200 mm, f/4), an intensified charged-coupled device (ICCD, PIMAX II, Princeton Instruments) mounted with a UV Nikon lens (105 mm, f/4.5) and different filters [i.e., 420 nm and 430 nm interference filters (IFs) with a full width at half maximum (FWHM) of 10 nm from Edmund Optics and a OG 550 long pass filter], a spectrometer (SP 2300i, Princeton Instruments), and a high-speed camera (Phantom 7.2, Vision Research) were employed to characterize the GA discharge in the N_2-CH_4 mixture. In the experiment, the gas mixture is ejected into the chamber through a small hole (3 mm) between the electrodes. The flow rates of N_2 and CH_4 are set to 10 standard liter per minute (SLPM) and 0.01 SLPM, respectively, and fixed even though the pressure changes. A current monitor (Pearson Electronics) and a voltage probe (Tektronix P6015A) are used to measure the waveforms of the current and the voltage simultaneously. The inset of Fig. 1 also shows a typical current-voltage waveform of the GA discharge in one discharge cycle and the current/voltage in several alternating periods. The frequency of the alternating current power supply is 35 kHz. The rated power of the high-voltage supply is manually set to 600 W, while the current and the voltage change automatically depending on the discharge conditions. The plasma initializes at the shortest gap between electrodes with current spikes. Later, the plasma column elongates driven by the jet flow. The current amplitude decreases slightly, while the voltage amplitude increases as the plasma column elongates. When the voltage reaches the breakdown threshold, re-ignition occurs at the shortest gap to start a new discharge cycle.

In the experiment, a glare from the GA discharge is detected when 0.1 vol. % CH_4 is mixed with nitrogen. Owing to this 0.1% CH_4 addition, the emission intensity is tenfold stronger than that from the discharge in pure N_2 gas. Because of this intense emission, the exposure time and the f-number of the digital camera are manually adjusted to avoid overexposure. Here, the exposure time was set to 1/8000 s and the f-number was 22. Figure 2 illustrates the images of the plasma column at 1–5 atm captured using the digital Nikon camera. A special layer around the purple GA column is identified in those images. This outer layer moves closer to the central discharge column as the pressure is increased. It should also be noted that this layer is not smoothly surrounding the plasma column. There seem some wrinkles or gaps in the layer, and so the color is inhomogeneous along the discharge column.

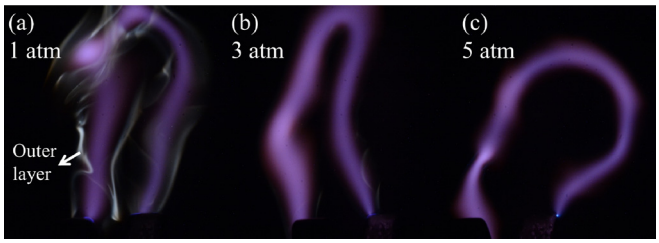

FIG. 2. Images of the GA column at 1–5 atm captured using the digital Nikon camera.

In order to gain more insights into this outer layer, the ICCD camera mounted with different filters was utilized to visualize the GA discharge channels. Figure 3 shows images captured with two bandpass interference filters (IF 420 nm, IF 430 nm) and a longpass filter (OG 550), together with the emission spectra in the relevant wavelength bands. By using the 420 nm interference filter, the strong emission from the plasma column is acquired without the apparent outer

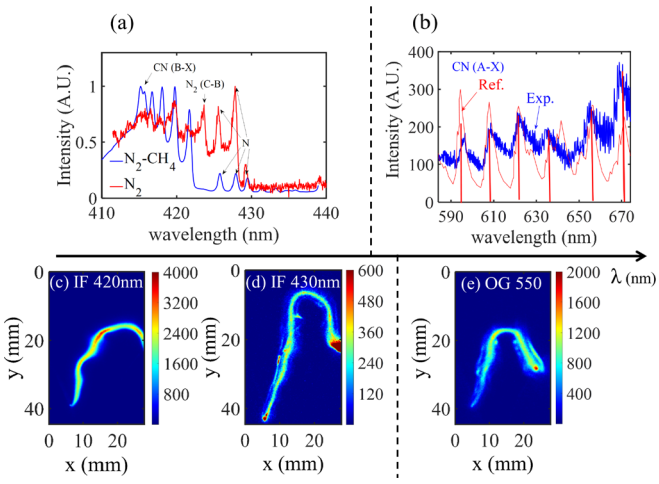

FIG. 3. Emission spectra and images captured with different filters. (a) Emission spectra of N_2-CH_4 and pure N_2 discharges in a wavelength range of 410–440 nm. (b) Emission spectra of N_2-CH_4 discharge in a wavelength range of 580–680 nm. (c) Image of N_2-CH_4 discharge captured with a 420 nm interference filter; the ICCD gate is 15 μs. (d) Image of N_2-CH_4 discharge captured with a 430 nm interference filter; the ICCD gate is 30 μs. (e) Image of N_2-CH_4 discharge captured with the OG 550 filter; the ICCD gate is 15 μs.

layer. However, the outer layer is distinctly detected by using the 430 nm interference filter and the OG 550 filter. The emission intensity of the outer layer detected with IF 420 nm is at least twenty times stronger than that of the plasma column detected with IF 430 nm. Meanwhile, the measured spectra indicate that in the wavelength range of 410 nm to 440 nm, only the emission from CN($B^2\sum^+$) and N atoms is clearly identified for the N_2-CH_4 discharge. Therefore, it can be confirmed that the emission signal acquired with IF 420 nm is mainly from the CN (B-X) transition, while the weak emission signal of the outer layer acquired with IF 430 nm is difficult to determine. The emission wavelength of atomic N is covered by the 430 nm interference filter, but the atomic N should be confined in the discharge channel, where the energetic electrons can dissociate nitrogen molecules and excite the N atoms. A more possible explanation is that the weak layered emission signal comes from the CH (A-X) transition, which has been detected when the methane concentration in nitrogen is higher.[25] Here, the CH (A) emission is too weak compared to that from CN (B) and thus not detected by the spectrometer. In the wavelength range of 570–680 nm, the CN ($A^2\prod_I - X^2\sum^+$) red emission is identified by comparison with the reported spectra.[27] Since the outer layer is detectable when the OG 550 filter is used, we can confirm the existence of CN (A) in the outer layer.

The dynamical behavior of this special outer layer around the GA discharge channel is acquired using a high-speed camera. Figure 4 displays snapshots of the moving discharge column at 1 atm. The outer layer closely surrounds the central plasma column throughout its movement. It also propagates further out from the discharge channel, as marked in Fig. 4. This rapid propagation may be due to the local thermal expansion and convection of the hot gas surrounding the gliding arc. However, when the outer layer moves too far away from the plasma column, it breaks up and becomes difficult to identify (see Fig. 4). Therefore, the outer layer is not smooth that in some segments of the plasma channel, it is distinguished with a sharp boundary, while in others, it is broken up and blurred. From the view point of dynamical behavior, this outer layer is similar to the flame front in combustion, which can propagate and extinguish. When the plasma column is re-ignited at the shortest gap between electrodes, the emission from the shortcut plasma column decays fast at a time scale of 0.4 ms, but the outer layer decays slower with a typical decay time of 1 ms. The slower vanishing of the outer layer infers that it is not directly controlled by the electric field.

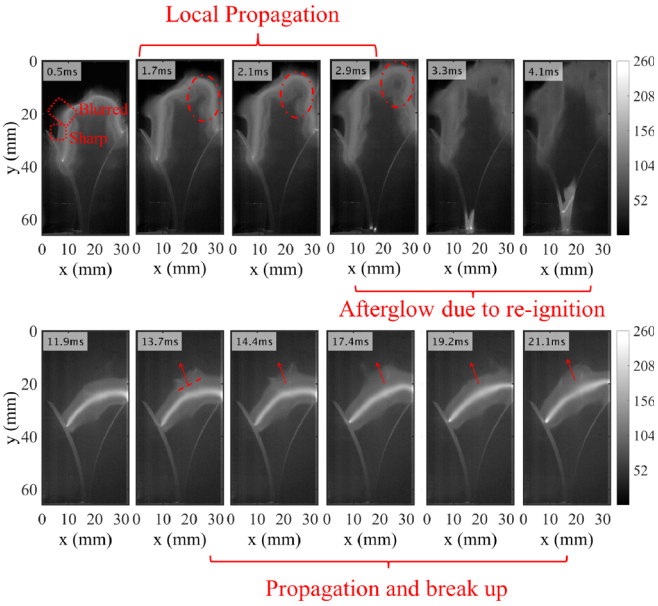

FIG. 4. Snapshots of the moving GA column and its outer layer.

This outer layer behaves similar to the flame front, and thus, a plasma-sustained radical propagation mechanism is proposed to explain the detected phenomena, in analogy with the flame front propagation mechanism. As illustrated in Fig. 5, the plasma column is located in the center, absorbing the externally input electrical power, and serves as a heat and radical source, while the surrounding is the cold N_2-CH_4 mixture. With the heat and radical species spreading out from the plasma column, the surrounding N_2-CH_4 mixture is heated up as well as mixes and reacts with the radicals from plasma. At the mixing layer, chemical reactions (see R1–R5 in Fig. 5)[21,22,25,28] including atomic N and excited N_2* could take place to form the excited CH, CN, etc., and emit their specific spectra. Here, the key point is the formation and transport of energetic species to support the chemical reactions of forming excited CN and CH species. In order to verify the formation of atomic species in the plasma column, thermodynamic analysis based on the assumption of chemical equilibrium is first performed. Since the temperature profile around the plasma column is crucial for the thermodynamic analysis, but it is difficult to measure, a simplified heating model is employed to simulate the temperature profiles around the plasma column. The governing equation of heat transfer is given by

$$\rho c_p \frac{\partial T_g}{\partial t} - \nabla \cdot k \nabla T_g = Q_{ht}, \tag{1}$$

where ρ is the gas density; c_p is the heat capacity at constant gas pressure; T_g is the gas temperature; k is the thermal conductivity; Q_{ht} denotes the heating power density. The heat capacity and the thermal conductivity as a function of temperature are obtained from the

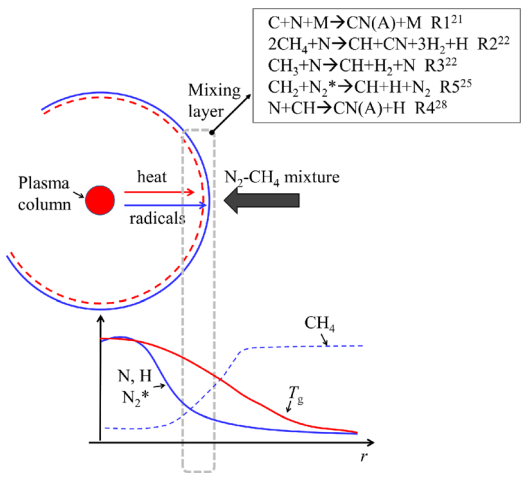

FIG. 5. A schematic of the mechanism of the outer layer formation around the plasma column.

database of the CEA (Chemical Equilibrium with Applications) program from NASA.[29] Q_{ht} is estimated according to the measured current and voltage as well as the length of the plasma column. In this work, the mean current reaches 290 mA and the input power density is around 4 kW per meter of the plasma column. With a presumed radius of 0.5 mm, the input power density in the plasma column is as high as 2.5×10^9 W/m^3. Assuming that all input energy converts into heat, the peak temperature is estimated to be around 5000 K in the plasma column, and the temperature drops with the increased radial distance from the plasma core. It should be noteworthy that the GA discharge is nonthermal, and so the temperature cannot be well defined. In the N_2 discharge, as we know, the input electrical energy is first transferred to the population of the vibrational states of nitrogen and later converts to heat through the V-T transition. It infers that the vibrational temperature should be higher than the translational temperature.[30] As a result, the effective temperature for chemical reactions is larger than the translational temperature due to the nonthermal properties. Actually, according to the emission spectra of CN (B-X) in the plasma column, the fitted vibrational temperature reaches 7000 K, higher than the peak temperature based on the thermal equilibrium. With the assumption of chemical equilibrium, the chemical species compositions with respect to temperature can be calculated using the CEA program. This indicates that in the center of the plasma column, the temperature (e.g., 5000 K) is extremely high so that gas species are partially decomposed into atoms (e.g., N, C, and H). Outside the plasma column, with the temperature decrease, the concentrations of those active atomic species naturally drop to form more stable species according to the chemical equilibrium calculation. However, there always needs some time to reach equilibrium, and at higher temperature, the lifetime of atomic species is longer. Hence, atomic species (mainly N and H) can transport out of the plasma column. The transport distance is basically determined by the local temperature and species. When enough energetic radical species can reach the mixing layer, highly exothermic chemical reactions occur to form the excited species. Since the energetic radical species are sustained by the plasma column and can be quickly consumed in the relatively cold gas, they cannot be further away from the plasma column. This is the underlying reason for the disappearance of the sharp layer when the layer propagates too far away from the plasma column, as demonstrated in Fig. 4.

The pressure effect on the layered structure can be explained by the fact that the gas density and heat capacity per volume increase with pressure. Thus, with a constant input power density, the hot volume around the plasma column naturally decreases with pressure. Furthermore, the atomic species can be consumed faster at higher pressure. Therefore, the outer layer can only exist closer to the plasma column at higher pressure.

In conclusion, the structure of the GA discharge column in the N_2-CH_4 mixture has been visualized using different detection schemes. A tenfold increment of emission intensity with the addition of 0.1% CH_4 in nitrogen is found. More importantly, a special layered structure around the GA discharge column has been detected. Imaging through spectral filters and spectral analysis indicate that this detected outer layer is basically due to the existence of CN (A) and CH (A). The separation of this outer layer to the plasma core decreases with pressure. Besides, it can propagate and extinguish, behaving similar to the flame front except that the flame is self-sustained by the fuel-oxidant reactions, while the outer layer is sustained by the plasma column. This outer layer is detected owing to the chemical reactions of energetic radical species from plasma and surrounding hydrocarbon compounds to form excited CH and CN species.

This work was financially supported by the Swedish Energy Agency, the Swedish Research Council, the Knut and Alice Wallenberg Foundation, and the European Research Council.

REFERENCES

[1]A. Fridman, A. Chirokov, and A. Gutsol, J. Phys. D: Appl. Phys. **38**, R1 (2005).
[2]A. Fridman, S. Nester, L. A. Kennedy, A. Saveliev, and O. Mutaf-Yardimci, Prog. Energy Combust. Sci. **25**, 211 (1999).
[3]J. J. Zhu, J. L. Gao, Z. S. Li, A. Ehn, M. Aldén, A. Larsson, and Y. Kusano, Appl. Phys. Lett. **105**, 234102 (2014).
[4]J. L. Gao, C. D. Kong, J. J. Zhu, A. Ehn, T. Hurtig, Y. Tang, S. Chen, M. Aldén, and Z. S. Li, Proc. Combust. Inst. **37**(4), 5629 (2019).
[5]Y. Kusano, J. J. Zhu, A. Ehn, Z. S. Li, M. Aldén, M. Salewski, F. Leipold, A. Bardenshtein, and N. Krebs, Surf. Eng. **31**(4), 282 (2015).
[6]H. Zhang, W. Z. Wang, X. D. Li, L. Han, M. Yan, Y. J. Zhong, and X. Tu, Chem. Eng. J. **345**, 67 (2018).
[7]W. Z. Wang, D. H. Mei, X. Tu, and A. Bogaerts, Chem. Eng. J. **330**, 11 (2017).
[8]Z. W. Sun, J. J. Zhu, Z. S. Li, M. Aldén, F. Leipold, M. Salewski, and Y. Kusano, Opt. Express **21**(5), 6028 (2013).
[9]J. J. Zhu, Z. W. Sun, Z. S. Li, A. Ehn, M. Aldén, M. Salewski, F. Leipold, and Y. Kusano, J. Phys. D: Appl. Phys. **47**(29), 295203 (2014).
[10]A. El-Zein, M. Talaat, G. El-Aragi, and A. El-Amawy, IEEE Trans. Plasma Sci. **44**(7), 1155 (2016).
[11]N. C. Roy, M. G. Hafez, and M. R. Talukder, Phys. Plasmas **23**(8), 083502 (2016).
[12]X. Tu, H. J. Gallon, and J. C. Whitehead, IEEE Trans. Plasma Sci. **39**(11SI1), 2900 (2011).
[13]N. C. Roy and M. R. Talukder, Phys. Plasmas **25**(9), 093502 (2018).
[14]Y. D. Korolev, O. B. Frants, V. G. Geyman, N. V. Landl, and V. S. Kasyanov, IEEE Trans. Plasma Sci. **39**(12SI1), 3319 (2011).
[15]O. Mutaf-Yardimci, A. V. Saveliev, A. A. Fridman, and L. A. Kennedy, J. Appl. Phys. **87**(4), 1632 (2000).
[16]S. Pellerin, F. Richard, J. Chapelle, J. M. Cormier, and K. Musiol, J. Phys. D: Appl. Phys. **33**(19), 2407 (2000).
[17]S. Kolev and A. Bogaerts, Plasma Sources Sci. Technol. **24**(1), 015025 (2015).
[18]G. Trenchev, S. Kolev, and A. Bogaerts, Plasma Sources Sci. Technol. **25**(3), 035014 (2016).
[19]S. R. Sun, S. Kolev, H. X. Wang, and A. Bogaerts, Plasma Sources Sci. Technol. **26**, 055017 (2017).
[20]A. F. Gutsol and S. P. Gangoli, IEEE Trans. Plasma Sci. **45**, 555 (2017).
[21]G. Dilecce, P. F. Ambrico, G. Scarduelli, P. Tosi, and S. De Benedictis, Plasma Sources Sci. Technol. **18**(1), 015010 (2009).
[22]J. Pereira, V. Massereau-Guilbaud, I. Geraud-Grenier, and A. Plain, Plasma Processes Polym. **2**(8), 633 (2005).
[23]C. D. Pintassilgo, J. Loureiro, G. Cernogora, and M. Touzeau, Plasma Sources Sci. Technol. **8**(3), 463 (1999).
[24]M. Kareev, M. Sablier, and T. Fujii, J. Phys. Chem. A **104**(31), 7218 (2000).
[25]H. Zhang, C. M. Du, A. J. Wu, Z. Bo, J. H. Yan, and X. D. Li, Int. J. Hydrogen Energy **39**(24), 12620 (2014).
[26]P. H. Joo, J. L. Gao, Z. S. Li, and M. Aldén, Rev. Sci. Instrum. **86**(3), 035115 (2015).
[27]N. Nishiyama, H. Sekiya, M. Tsuji, and Y. Nishimura, Rep. Inst. Adv. Mater. Study **1**, 35–50 (1987).
[28]D. W. Setser and B. A. Thrush, Nature **200**(490), 864 (1963).
[29]S. Gordon and B. J. McBride, NASA Reference Publication Report No. 1311, 1996.
[30]C. D. Kong, J. L. Gao, J. J. Zhu, A. Ehn, M. Aldén, and Z. S. Li, Phys. Plasmas **24**(9), 093515 (2017).